Cancer Research

KRAS Genomic Status Predicts the Sensitivity of Ovarian Cancer Cells to Decitabine

Michelle L. Stewart[1], Pablo Tamayo[1], Andrew J. Wilson[2], Stephanie Wang[1], Yun Min Chang[1], Jong W. Kim[1], Dineo Khabele[2], Alykhan F. Shamji[1], and Stuart L. Schreiber[1]

Abstract

Decitabine, a cancer therapeutic that inhibits DNA methylation, produces variable antitumor response rates in patients with solid tumors that might be leveraged clinically with identification of a predictive biomarker. In this study, we profiled the response of human ovarian, melanoma, and breast cancer cells treated with decitabine, finding that RAS/MEK/ERK pathway activation and DNMT1 expression correlated with cytotoxic activity. Further, we showed that *KRAS* genomic status predicted decitabine sensitivity in low-grade and high-grade serous ovarian cancer cells. Pretreatment with decitabine decreased the cytotoxic activity of MEK inhibitors in *KRAS*-mutant ovarian cancer cells, with reciprocal downregulation of DNMT1 and MEK/ERK phosphorylation. In parallel with these responses, decitabine also upregulated the proapoptotic BCL-2 family member BNIP3, which is known to be regulated by MEK and ERK, and heightened the activity of proapoptotic small-molecule navitoclax, a BCL-2 family inhibitor. In a xenograft model of *KRAS*-mutant ovarian cancer, combining decitabine and navitoclax heightened antitumor activity beyond administration of either compound alone. Our results define the RAS/MEK/DNMT1 pathway as a determinant of sensitivity to DNA methyltransferase inhibition, specifically implicating *KRAS* status as a biomarker of drug response in ovarian cancer. *Cancer Res; 75(14); 2897–906. ©2015 AACR.*

Introduction

DNA methylation plays an active role in chromatin structure and gene expression and thus can significantly affect tumorigenicity (1–3). Decitabine is a cancer therapeutic that disrupts DNA methylation through inhibition of DNA methyltranferases, DNMT1, DNMT3A, and DNMT3B (3). Decitabine is approved to treat hematologic malignancies and in this context provides significant therapeutic benefit. Indeed, low-dose decitabine induced an objective response in 73% of patients with myelodysplasic ($n = 77$) and chronic myelomonocytic leukemia ($n = 18$; ref. 4). Although the best clinical response occurred in patients who showed rapid hypomethylation in peripheral blood and bone marrow cells, the degree of hypomethylation failed to correlate with response (4).

In contrast to hematopoietic cancers, decitabine shows moderate to low response rates in patients with solid tumors. Treatment with low-dose decitabine in patients with female reproductive ($n = 35$), melanoma ($n = 23$), and breast ($n = 4$) cancers demonstrated a combined response and stable disease count of 6%, 26%, and 50%, respectively (2). Identifying stratification markers as well as optimal combination strategies for decitabine treatment may enhance this compound's clinical benefit in patients with solid tumors.

Small-molecule sensitivity profiling of deeply characterized cancer cell lines is one approach to identify features that correlate with compound activity (5–8). For example, profiling experiments clearly identify the enhanced sensitivity of *BRAF*-mutant cells to BRAF inhibitors, and this association predicts response in patient populations (6–8). To date, sensitivity-profiling experiments have relied on 3-day time points to measure viability. However, small molecules that target chromatin-modifying proteins are reported to decrease cellular viability at extended time points (9, 10). As such, longer time points may be more informative in studying dependencies targeted by chromatin-modifying agents, such as decitabine.

Here, we used a 9-day viability assay to demonstrate that a subset of solid tumor cell lines is sensitive to low-dose decitabine at clinically achievable concentrations. We showed that RAS/RAF/MEK pathway activation as well as DNMT1 expression correlates with sensitivity to decitabine. We demonstrated that mutation or amplification of *KRAS* predicts sensitivity to decitabine in ovarian cancer cell lines. We further observed changes in activity of navitoclax and MEK inhibitors following decitabine pretreatment and showed that BCL-2 and MEK signaling may regulate decitabine's activity in RAS-activated cancer cell lines. Finally, we showed that the combination of decitabine and navitoclax significantly decreased tumor volume to a greater extent than either agent alone in a cell line–derived xenograft model.

Materials and Methods

Reagents and cell lines

All cell lines were obtained from the Broad Institute Biological Samples Platform (BSP) or ATCC. All cell lines were purchased in 2012 and cultured as previously described (6). Cell line profiling

[1]The Broad Institute of Harvard and MIT, Cambridge, Massachusetts. [2]Department of Obstetrics and Gynecology, Vanderbilt University, Nashville, Tennessee.

Note: Supplementary data for this article are available at Cancer Research Online (http://cancerres.aacrjournals.org/).

Corresponding Author: Stuart L. Schreiber, Broad Institute, 415 Main Street, Cambridge, MA 02142. Phone: 617-714-7081; Fax: 617-714-8969; E-mail: stuart_schreiber@harvard.edu

doi: 10.1158/0008-5472.CAN-14-2860

was performed within 6 months of receiving the cell lines. The cell lines were authenticated by BSP or ATCC via SNP array and short-tandem repeat profiling, respectively. Authentication of the cell lines after purchasing was not performed. Mutation and gene expression data for each cell line were obtained from the Cancer Cell Line Encyclopedia (8). Antibodies were purchased from Cell Signaling Technology. DNMT3B antibody was purchased from Abcam. All compounds were dissolved in DMSO and stored at −20°C. For all 6- and 9-day treatments, media and compound were replenished every 3 days.

Cell viability

Cell density was optimized in 384-well plates for 3- or 9-day treatment independently using CellTiter-Glo (Promega) per the manufacturer's instructions (30 μL). Cell density was optimized such that cell growth for the duration of the treatment fell within the linear range. For cotreatment combination studies, cells were plated at a density of 250 cells per well in 96-well plates (100 μL). Cells were plated and allowed to adhere for 24 hours prior to administering the compound. Cell viability was measured using CellTiter-Glo (1:2 with PBS) per the manufacturer's instructions. Luminescence was measured using the Envision (Perkin Elmer). Background luminescence was subtracted, and the measured ATP level was normalized to the vehicle. For all 6- and 9-day treatments, media and compound were replenished every 3 days.

Capase-3/7 activation

Cells were plated at a density of 250 cells per well in 96-well plates and allowed to adhere for 24 hours prior to treatment. Cells were treated for 6 days with decitabine. CellTiter Blue (Promega) and Caspase Glo (Promega) were used in combination per the manufacture's instructions. Fluorescence ($560_{Ex}/590_{Em}$ nm) and luminescence were measured using the SpectraMax M5 (Molecular Devices). Background luminescence was subtracted, and the measured caspase activation was normalized to cell number. For all 6-day treatments, media and compound were replenished every 3 days.

Western blot analysis

Cells were lysed in RIPA buffer (Thermo) supplemented with PhosphoStop (Roche) and complete protease inhibitor (Roche). Lysate (50 μg) was loaded onto a NuPage Bis–Tris Gel (4%–12%; Invitrogen) and transferred using the iBlot (Invitrogen). The membrane was blocked (5% milk/PBS/0.1% Tween) and incubated with primary antibody (3% BSA/PBS/0.1% Tween) overnight at 4°C or at room temperature for 2 hours. The membrane was washed three times (0.1% Tween/PBS) and incubated with the appropriate secondary antibody (3% BSA/PBS/0.1% Tween). Luminescence was captured after the addition of FemtoSubstrate (Thermo) using the Image Station 4000 MM (Kodak) and Carestream MI software at various exposure times. Quantification of the Western blots was performed using ImageJ.

Pretreatment combination studies

Cells ($0.1–0.25 \times 10^6$) were plated in 100-cm^2 dishes. After 24 hours, cells were treated with decitabine (0.5 μmol/L) or DMSO for 3, 6, or 9 days. Cell density was adjusted every 3 days to prevent overgrowth, and the media and compound treatment were replaced. Viable cells were harvested by trypsin and plated (30 μL) in 384-well plates in the presence of decitabine or DMSO at an optimized density and allowed to adhere for 24 hours. Combination compounds (100 nL) were administered for 72 hours, and cell viability was measured as described (11). Viability was normalized to the cell state tested, and the area under the curve (AUC) was determined for treatment with decitabine ($AUC_{dectabine}$) or DMSO (AUC_{DMSO}) as previously described (6). Cell viability of decitabine or DMSO pretreated cells was confirmed by calcein AM staining.

Correlation analysis using differential mutual information

We used an estimator of the differential mutual information

$$I(x,y) = \iint P(x,y) log\left(\frac{P(x,y)}{P(x)P(y)}\right) dxdy, \quad (1)$$

where x is the activity to decitabine profile and y is each of the genomic alterations or pathway profiles being compared against. The computation is based on kernel density estimation following a methodology similar to that used in Wood and colleagues but normalizing the mutual information (12, 13) as to produce an information coefficient,

$$I_c(x,y) = \text{sign}(\rho(x,y)(1 - e^{-2I(x,y)})^{1/2}. \quad (2)$$

To assess the significance of every I_c score, we perform a permutation test randomly permuting the activity to decitabine profile and based on those scores compute nominal P values and false discovery rates (FDR) as those shown in Supplementary Tables S1 and S2.

Database of gene sets

The database of gene sets used in this study (7,762 gene sets) consists of the Molecular Signatures Database (MSigDB, release 4.0, www.broadinstitute.org/msigdb) subcollections c2, c3, c5, and c6 (14), plus a preliminary unpublished collection of oncogenic signatures that will be incorporated in subcollection c6 in a forthcoming release of MSigDB.

Xenograft assay

Four- to 5-week-old female athymic Nude-*Foxn1*^{nu} mice were purchased from Harlan Laboratories and maintained in sterile housing throughout the experimental period. For this subcutaneous (s.c.) xenograft model, 5×10^6 OVCAR8 cells in 200 μL of a PBS/Matrigel (BD Biosciences) mixture (1:1 v/v) were injected s.c. into the right flank of the mice. After the tumors reached approximately 200 mm^3 in volume, mice were randomized and treated with decitabine (0.2 mg/kg s.c. thrice weekly), navitoclax (100 mg/kg i.p. five times per week), decitabine and navitoclax as described or vehicle control (PBS) for 4 weeks before euthanasia and necropsy. Week 4 treatment of the combination study omitted one injection of decitabine and two injections of navitoclax in all cohorts. Groups of 7 mice were used. Tumor volume was calculated weekly from caliper measurements of the smallest (SD) and largest tumor diameter (LD) using the formula: volume = $[LD \times SD^2] \times \pi/6$. Experiments performed received prior approval from the Vanderbilt University Institutional Animal Use and Care Committee, and all animals were maintained in accordance with guidelines of the American Association of Laboratory Animal Care.

Combined bisulfite restriction analysis

Cells were treated for 6 days with decitabine (0.5 μmol/L) or DMSO. Cell lysis and bisulfite treatment was accomplished using the EpiTect Plus LyseAll Lysis Kit and the EpiTect Plus Bisulfite Kit

by Qiagen as per the manufacturer's instructions. Combine bisulfite restriction analysis was performed as previously described (15). Briefly, PCR was carried out using HotStarTaq DNA polymerase (Qiagen) as per the manufacturer's instructions using bisulfite-treated DNA (300 ng). Touchdown PCR was performed using BNIP3 primers surrounding the transcriptional start site F: 5′-TTYGGTYGGAGGAATTTATAGGGTAG, R: 5′-CCCTCRCCCA-CCRCCAAAAC (where Y = C or T and R = A or G; temperature cycle: 58–3, 56–4, 54–5, 52–26). The 156-bp PCR product (10 μL) was digested with the restriction enzyme AfaI (Invitrogen) for 1 hour at 37°C, and the DNA was subjected to 2% agarose gel electrophoresis and imaged.

Results

Decitabine decreases cell viability in a time-dependent manner in a subset of solid tumor cell lines

To study the effects of compounds that lead to changes in chromatin modifications, we used a 9-day viability assay. We targeted two distinct chromatin modifications, DNA methylation and histone deacetylation, using the FDA-approved small-molecule therapeutics, decitabine and vorinostat, in an ovarian cancer cell line (OVCAR8). Media and compound were replaced every 3 days to minimize nutrient deprivation and compound degradation. Although both compounds showed a dose-dependent decrease in viability, decitabine showed a marked change in activity over time. Specifically, activity improved approximately 1,000-fold from 3 days ($IC_{50}^{day\ 3}$, > 33.3 μmol/L) to 9 days of treatment ($IC_{50}^{day\ 9}$, 22.2 nmol/L). In contrast, treatment with vorinostat caused a stable decrease in cell viability at all three time points (Fig. 1A).

To understand better decitabine's activity in solid tumors, we profiled the response of 45 cancer cell lines in ovarian, melanoma, and breast lineages over 9 days of treatment with decitabine. In general, decitabine showed no activity at 3 days of treatment, but significantly decreased cell viability at 6 and 9 days of treatment (Fig. 1B). A subset of cell lines in all three lineages showed substantial sensitivity to low doses of decitabine at 9 days of treatment (IC_{50} < 150 nmol/L), and decitabine elicited a dynamic range in sensitivity greater than 1,000-fold (10 nmol/L > IC_{50} > 10 μmol/L) in all lineages after 9 days of treatment (Supplementary Fig. S1).

KRAS mutation status predicts decitabine sensitivity in ovarian cancer cell lines

We correlated genomic alterations and pathway features to decitabine sensitivity and resistance in an unbiased manner using a differential mutual information estimator (see Materials and Methods). We found that activating mutations in *KRAS* (P 1.88×10^{-2}) and *NRAS* (P 7.43×10^{-2}), but not *BRAF*, strongly correlate with sensitivity to decitabine. Amplifications in *CRAF* ($P = 7.65 \times 10^{-2}$), a downstream effector of RAS proteins, also correlated with sensitivity. Seven of the 10 most sensitive cell lines contained genomic alterations in *KRAS* or *CRAF*, and the most sensitive cell lines were *KRAS*-mutant ovarian cancer cell lines ($n = 4$; Fig. 2A and Supplementary Table S1).

We also found that genomic alterations in genes associated with the activation of p38 signaling correlated with resistance to decitabine. Specifically, amplification of *MAP2K6* ($P = 1.9 \times 10^{-3}$), which activates p38 signaling, and deletion of genes that inactivate p38 signaling, such as *USP47* ($P = 1.4 \times 10^{-3}$) and *DUSP26* ($P = 1.0 \times 10^{-3}$), correlated with resistance to decitabine (Supplementary Table S1). Activation of p38 signaling is reported to oppose RAS-induced cancer cell proliferation (16, 17) and may represent a distinguishing feature of cancer cell lines that are resistant to decitabine. To mitigate confounding variables, we analyzed doubling time for each cell line. Importantly, sensitivity to decitabine failed to correlate with doubling time (Supplementary Fig. S2A).

Global gene-expression profiles available from the Cancer Cell Line Encyclopedia (8) were analyzed to score the activity of gene sets (see methods) that represent defined pathways for each cell line using single-sample Gene Set Enrichment Analysis (18). These enrichment scores were correlated to decitabine sensitivity using the differential mutual information estimator to identify pathways implicated in the response to decitabine. Consistent with their association to genomic alterations in RAS pathway genes, sensitivity to decitabine also correlated with gene-set signatures derived from overexpression of *KRAS* (KRAS. Breast_HMLE.24_UP, $P = 2.46 \times 10^{-3}$), *CRAF* (RAF_UP.V1_DN, $P = 2.40 \times 10^{-3}$) and *MEK* (MEK_UP.V1_DN, $P = 2.40 \times 10^{-2}$; Fig. 2B). High expression of genes in gene-set signatures corresponding to cell-cycle regulation (Mitotic_Cell_Cycle_Checkpoint, $P = 5.19 \times 10^{-4}$, Cell_Cycle_Go_0007049, $P = 7.78 \times 10^{-4}$) also strongly correlated with sensitivity to decitabine (Supplementary Table S2).

Given the impact of RAS/RAF/MEK signaling on decitabine activity, we hypothesized that *KRAS* genomic status may predict sensitivity to decitabine in ovarian cancer. Clinically, *KRAS* mutations occur in approximately 30% of low-grade serous ovarian cancers, and *KRAS* amplifications occur in approximately 11% of high-grade serous ovarian cancers (19). We profiled an additional low-grade *KRAS*-mutant (*TP53* wild-type), two high-grade *KRAS*-mutant (*TP53*-mutant), and three high-grade *KRAS*-amplified (*TP53*-mutant) serous ovarian cancer cell lines. Low-grade and high-grade ovarian cancer cell lines that harbored mutations or genomic amplifications in *KRAS* were highly sensitive to decitabine (IC_{50} < 150 nmol/L) compared with *KRAS* wild-type ovarian cancer cell lines (Fig. 2C). This sensitivity is consistent with decitabine's activity in the previously profiled *KRAS*-mutant ovarian cancer cell lines. To extend these finding to other lineages, we tested the activity of decitabine against a limited panel of pancreatic and colon cancer cell lines. All four pancreatic cell lines tested harbor a G12 mutation in *KRAS* and were sensitive to decitabine after 9 days of treatment. The IC_{50} values for the pancreatic cell lines PANC1, KP2, L33, and SNU213 were 267.2 nmol/L, 75.2 nmol/L, 61.29 nmol/L, and 15 nmol/L, respectively (Supplementary Fig. S2B). In contrast, *KRAS* mutation status failed to predict sensitivity to decitabine in colon cancer; although two *KRAS*-mutant cell lines (HCT116, RCM) were sensitive to decitabine, two (HCT15, LS513) displayed moderate sensitivity and one (SNUC2A) was resistant (Supplementary Fig. S2C).

DNMT1 plays a role in mediating decitabine's activity in cancer cell lines

Decitabine targets DNA methyltransferases DNMT1, DNMT3A, and DNMT3B. Given the role of DNMT1 as a downstream effector of RAS proteins (20, 21), we analyzed basal gene-expression levels available from the Cancer Cell Line Encyclopedia (8) and changes in protein levels of DNA methyltransferases after treatment with decitabine. Decitabine sensitivity correlated more strongly with high expression of *DNMT1* (ρ, −0.443) than *DNMT3A* (ρ, −0.176) or *DNMT3B* (ρ, 0.187) as assessed by Pearson regression analysis (Fig. 3A and Supplementary Fig. S3A). In addition, decitabine clearly decreased DNMT1 levels in three *KRAS*-mutant ovarian cancer cell lines, OVCAR8, TOV21G, and OV56 (Fig. 3B

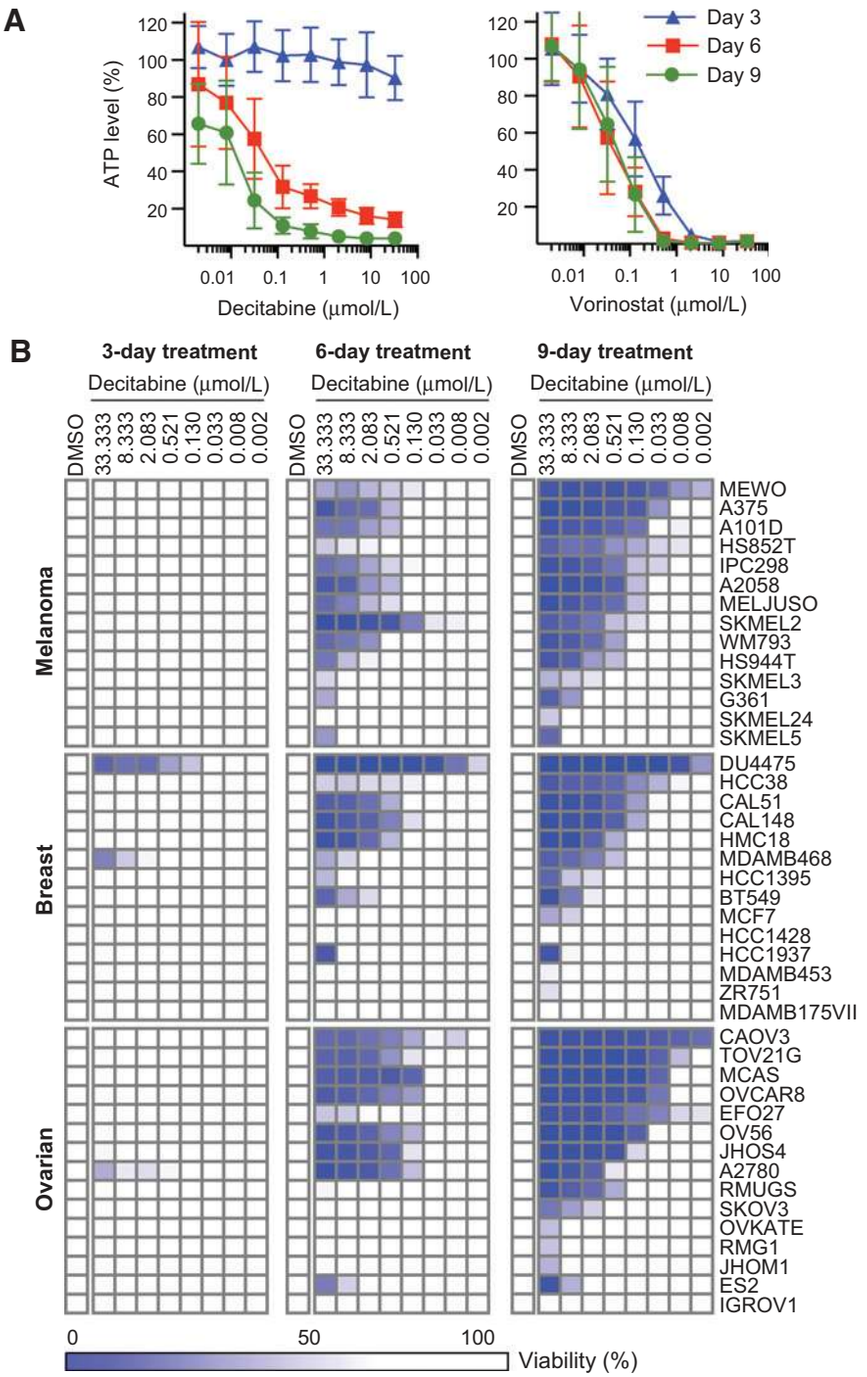

Figure 1.
Decitabine decreases cell viability in a time-dependent manner in a subset of cancer cell lines. A, cell viability was measured after treatment with decitabine (left) or vorinostat (right) in OVCAR8 cells. Data are representative of two independent experiments (14 replicates; mean ± SD). B, cell viability was measured for a panel of 45 solid tumor lines after treatment with decitabine. Data are representative of two independent experiments, each measured in 14 replicates (mean).

and Supplementary Fig. S3B). The DNMT3A protein level remained constant in all three cell lines, and DNMT3B protein level decreased only in OV56. *KRAS* wild-type ovarian cancer cell lines displayed a varied response to decitabine (Supplementary Fig. S3B).

Given our observed connection between RAS/RAF/MEK pathway activation and DNMT1, we investigated the impact of MEK inhibition on DNMT1 protein levels. As such, we observed that treatment with selumetinib, a small-molecule inhibitor of MEK, decreased DNMT1 protein levels in two *KRAS*-mutant ovarian cancer cell lines (Fig. 3C and Supplementary Fig S3C). This observation is in accordance with the reported regulation of DNMT1 protein levels by the RAS/RAF/MEK signaling cascade (22).

Pretreatment with decitabine alters the activity of a subset of small-molecule probes

We used combination profiling to interrogate further the mechanism of action of decitabine in a panel of 34 decitabine-sensitive and decitabine-resistant cell lines. To determine the

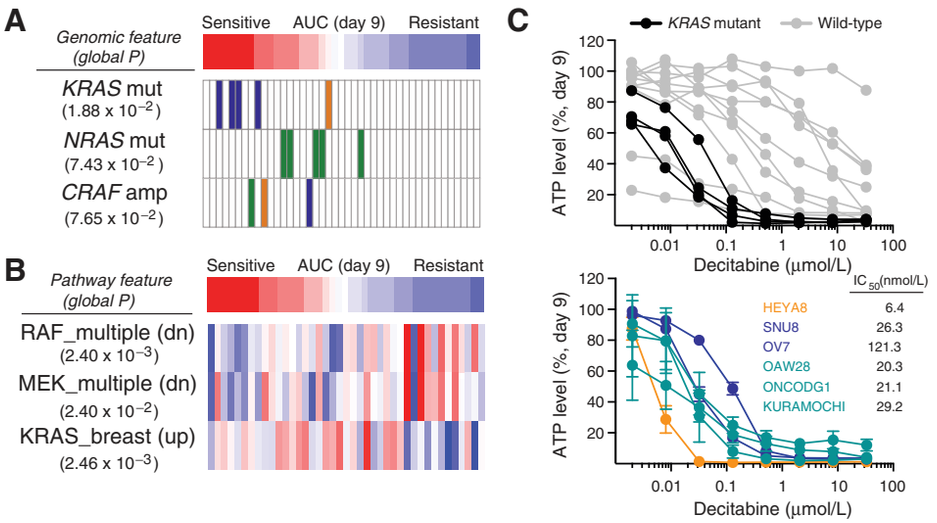

Figure 2.
KRAS genomic status predicts decitabine sensitivity in ovarian cancer cell lines. A, correlation analysis based on differential mutual information was used to correlate the cellular response of decitabine (9-day treatment) with genomic features of ovarian (blue), melanoma (green), and breast (orange) cancer cell lines. B, correlation analysis based on differential mutual information was used to correlate the cellular response of decitabine (9-day treatment) with pathway features as defined by gene sets with high gene expression (red) or low gene expression (blue). C, cell viability after 9 days of treatment with decitabine are shown for the profiled *KRAS*-mutant (black) and wild-type (gray) ovarian cancer cell lines. Cell viability was measured in one additional *KRAS*-mutant low-grade serous ovarian cancer cell line (orange), two additional *KRAS*-mutant high-grade serous ovarian cancer cell lines (navy), and three additional *KRAS*-amplified high-grade serous ovarian cancer cell lines (teal). Data are representative of two independent experiments (14 replicates; mean ± SD).

appropriate combination schedule, we measured the change in activity of the histone deacetylase inhibitor vorinostat, a compound known to synergize with decitabine (23). The human plasma maximum concentration (C_{max}) value ranges from 0.3 to 1.6 μmol/L for low-dose decitabine treatment (24), and, thus, a clinically meaningful concentration of decitabine (0.5 μmol/L) was chosen for all combination experiments. For cotreatment experiments, A375 cancer cells were treated for 3 days with vorinostat and low-dose decitabine (0.5 μmol/L), and cell viability was measured. For pretreatment experiments, A375 cancer cells were pretreated with low-dose decitabine (0.5 μmol/L) for 9 days and live cells, as verified by staining with calcein AM, were treated with decitabine and vorinostat for 3 days. Pretreatment with decitabine, but not cotreatment, increased activity of vorinostat (Fig. 4A).

Next, we measured the change in activity of a combination "informer set" consisting of 38 small molecules with varying mechanisms of action after pretreatment with low-dose decitabine (0.5 μmol/L) for 9 days followed by coadministration of decitabine and the combination "informer set." Although the majority of compounds responded in a similar manner, a number of significant changes in compound activity were observed upon pretreatment with decitabine (Fig. 4B). Specifically, our data confirmed that decitabine pretreatment increased activity of HDAC inhibitors in a number of solid tumor cell lines. In addition, pretreatment with decitabine increased the activity of the BCL-2 family inhibitor, navitoclax, and decreased activity of MEK inhibitors, such as trametinib and selumetinib, and DNA targeting agents (Fig. 4C). The decrease in activity of DNA-targeting agents, which require cell division to induce cell death, is

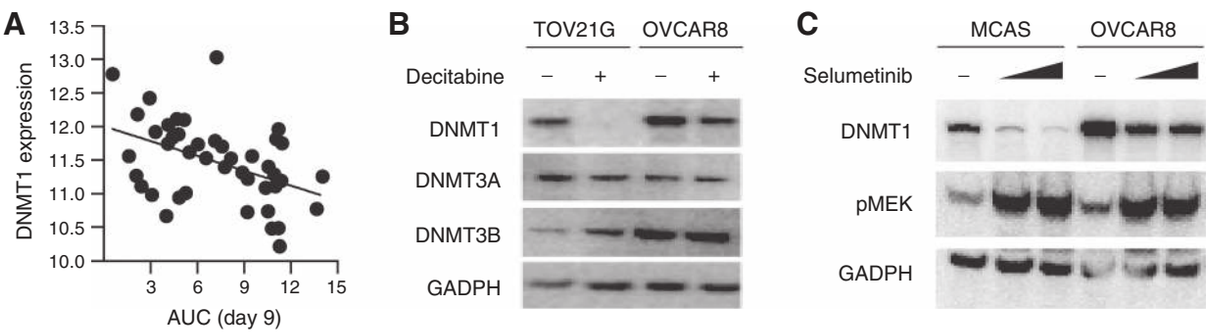

Figure 3.
DNMT1 plays a role in mediating decitabine's activity. A, cell viability after treatment with decitabine (AUC, *x*-axis) was plotted against DNMT1 mRNA expression (log_2, *y*-axis). B, Western blot analysis was performed after treatment with decitabine (0.5 μmol/L) or DMSO for 9 days in two *KRAS*-mutant ovarian cancer cell lines. C, DNMT1 protein level was probed by Western blot after treatment with selumetinib for 6 days in two *KRAS*-mutant ovarian cancer cell lines. Data are representative of two independent experiments.

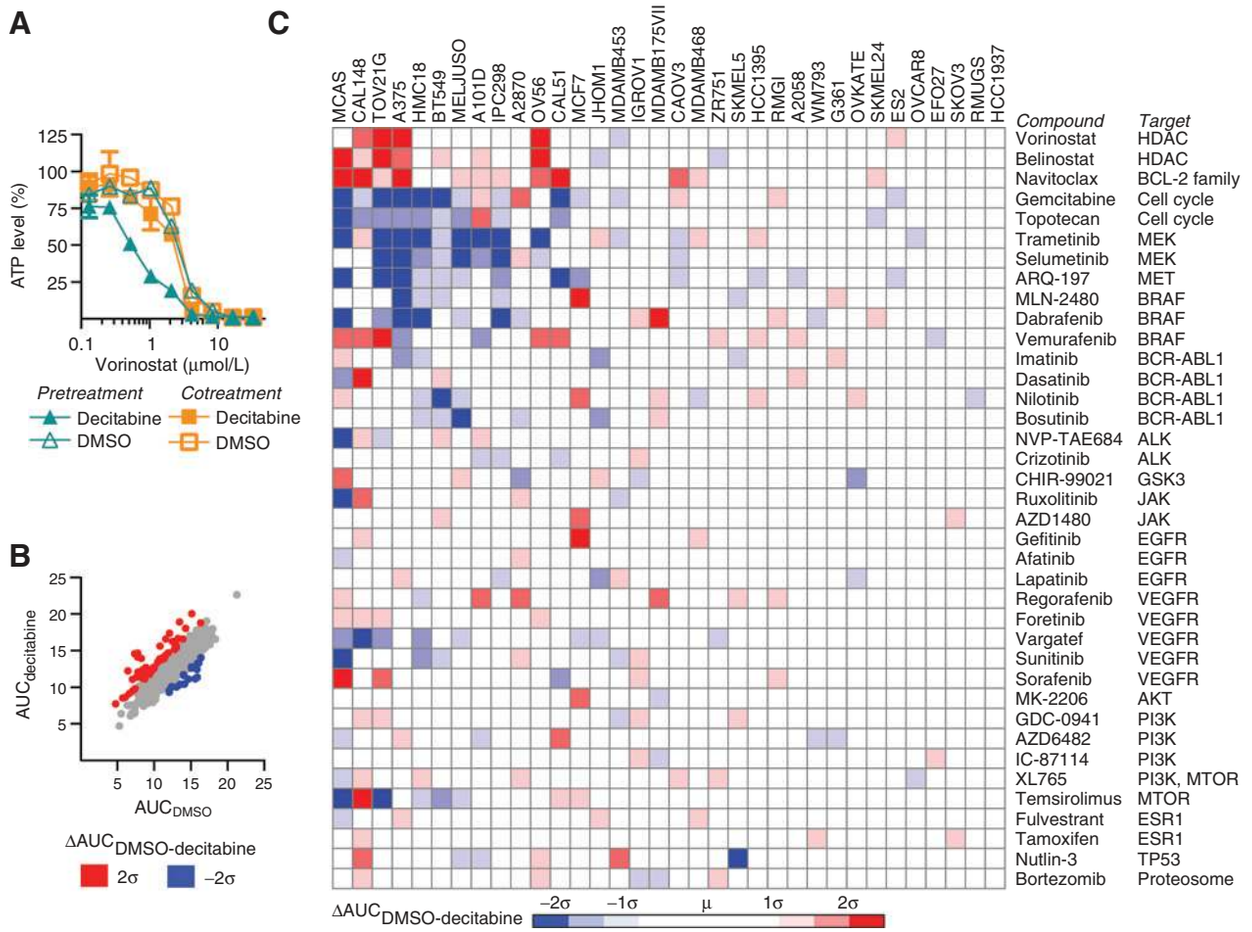

Figure 4.
Pretreatment with decitabine alters the activity of a subset of small-molecule probes. A, cell viability was measured after cotreatment with vorinostat and decitabine for 3 days or after pretreatment with decitabine or DMSO for 9 days followed by cotreatment with vorinostat and decitabine for 3 days (two biological replicates, mean ± SD). B, thirty-four cancer cell lines were pretreated with decitabine (0.5 μmol/L) or DMSO for 9 days. Viable cells were harvested and cotreated with decitabine (0.5 μmol/L) or DMSO and the combination "informer set." Cell viability was measured after 3 days and normalized to the cell state tested. The AUC was determined for treatment with decitabine ($AUC_{decitabine}$, *y*-axis) or DMSO (AUC_{DMSO}, *x*-axis). Data are the mean of two biological replicates. C, the difference between $AUC_{decitabine}$ and AUC_{DMSO} was plotted for each cell line (*x*-axis) and each "informer set" compound (*y*-axis).

consistent with the reported observation that decitabine can induce a quiescent cell population in certain contexts (25). Importantly, the majority of compounds, including GDC-0941 (pan-PI3K inhibitor), bortezomib (proteasome inhibitor), and NVP-TAE684 (ALK inhibitor), showed no change in activity after pretreatment with decitabine despite showing activity as single agents (Fig. 4C and Supplementary Fig. S4A). Together, our data suggest that decitabine induces an altered cell state characterized by decreased sensitivity to MEK inhibitors and increased sensitivity to HDAC and BCL-2 family inhibitors. We hypothesize that MEK/ERK and BCL-2 family signaling may play a direct role in mediating decitabine sensitivity.

Decitabine modulates sensitivity to MEK inhibitors in KRAS-mutant ovarian cancer cell lines

We investigated the relationship between *KRAS* status and changes in sensitivity to the MEK inhibitor trametinib after pretreatment with decitabine. We observed that ovarian cancer cell lines harboring a mutation in *KRAS* had a decreased response to trametinib after pretreatment with decitabine (Fig. 5A). We assessed the time point at which pretreatment with decitabine altered compound activity. We found that pretreatment with decitabine for 3 days, followed by cotreatment with decitabine and trametinib for 3 days, induced changes in compound sensitivity comparable to decitabine pretreatment for 9 days in a *KRAS*-mutant ovarian cancer cell line (MCAS) and a *CRAF*-amplified melanoma cell line (A375; Fig. 5B and Supplementary Fig. S4B).

Re-activation of the MEK/ERK pathway as demonstrated by phosphorylation of MEK and ERK has been shown to reduce activity of MEK inhibitors (26). As such, we examined the effect of decitabine treatment on phosphorylation of MEK and ERK. Decitabine treatment for 6 days increased phosphorylation of both MEK and ERK in a *KRAS*-mutant ovarian cancer cell line (MCAS), but not a lineage-matched *KRAS* wild-type cell line (RMGI; Fig. 5C and Supplementary Fig. S5A). Decitabine also increased phosphorylation of MEK in OVCAR8, a high-grade serous ovarian cancer cell line that harbors a mutation in *KRAS* (Supplementary Fig. S5B).

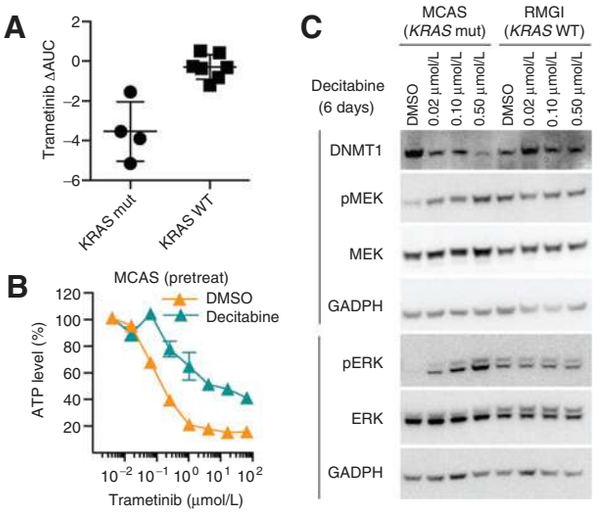

Figure 5.
Decitabine modulates MEK/ERK pathway activation. A, change in activity of the MEK inhibitor trametinib after pretreatment for 9 days with decitabine in *KRAS*-mutant and *KRAS* wild-type ovarian cancer cell lines. B, *KRAS*-mutant ovarian cancer cell line, MCAS, was pretreated with decitabine for 3 days, followed by cotreatment with decitabine and trametinib for 3 days (two biological replicates; mean ± SD). Data were normalized to the ATP levels (CTG) measured for the corresponding DMSO- or decitabine-treated controls (6 days). C, phosphorylation of MEK and ERK was probed by Western blot after treatment with decitabine for 6 days in a *KRAS*-mutant (MCAS) and *KRAS* wild-type (RMGI) ovarian cancer cell line. Data are representative of two independent experiments.

Decitabine modulates sensitivity to the BCL-2 family inhibitor, navitoclax, in KRAS-mutant ovarian cancer cell lines

We confirmed that pretreatment with decitabine increases sensitivity to the BCL-2 family inhibitor navitoclax. Specifically, we observed that pretreatment with decitabine for 3 days followed by cotreatment with decitabine and navitoclax for 3 days increased activity of navitoclax in a *KRAS*-mutant ovarian cancer cell line (MCAS; Fig. 6A). In an effort to simplify dosing and scheduling, we assessed the effect of cotreatment with decitabine and navitoclax. Cotreatment with decitabine increased activity of navitoclax in MCAS and OVCAR8 cell lines (Fig. 6B and Supplementary Fig. S5C). Interestingly, decitabine cotreatment (Fig. 6B), but not pretreatment (Fig. 4C), increased sensitivity to navitoclax in OVCAR8, a high-grade serous ovarian cancer.

Activation of the MEK/ERK pathway has previously been shown to increase expression of the BCL-2 family proapoptotic protein, BNIP3 (27–29). Consistent with this report, we found that decitabine treatment for 6 days increased expression of BNIP3 in MCAS and OVCAR8, *KRAS*-mutant ovarian cancer cell lines, but not in RMGI, a *KRAS* wild-type ovarian cancer cell line after treatment for 6 days (Fig. 6C). In addition, decitabine treatment for 6 days decreased methylation at the transcriptional start site of *BNIP3* in MCAS (Supplementary Fig. S5D). Given the role of *BNIP3* as a proapoptotic BCL-2 family member, we measured activation of caspase-3 and -7 as a marker for apoptosis after decitabine treatment for 6 days. Decitabine induced a dose-dependent increase in caspase activation at time points corresponding to decreased cell viability in both MCAS and OVCAR8 (Fig. 6D). Together, these data suggest that MEK/ERK activation and upregulation of BNIP3 may play a role in mediating decitabine sensitivity in *KRAS*-activated ovarian cancer cell lines and provide a strong rationale for combining decitabine and navitoclax in this cancer context.

The combination of decitabine and navitoclax shows activity in a xenograft model derived from a KRAS-mutant ovarian cancer cell line

To extend these findings *in vivo*, we first tested the response of a *KRAS*-mutant ovarian cell line (OVCAR8) to decitabine as a single agent in a murine xenograft model. We used a subcutaneous OVCAR8 xenograft model, which displayed slower growth than an intraperitoneal xenograft and allowed for extended treatment with decitabine. Decitabine was administered at low doses as previously reported for 4 weeks following initial tumor formation (0.2 mg/kg s.c., 3× per week; ref. 30). Low-dose decitabine displayed a moderate decrease in tumor volume (Fig. 7A) and tumor mass (Supplementary Fig. S6A). No overt toxicities were observed.

We next tested the effect of coadministration of decitabine and navitoclax in a murine xenograft model using OVCAR8. Decitabine (0.2 mg/kg s.c., 3× per week) and navitoclax (100 mg/kg i.p., 5× per week) were administered alone or in combination for 4 weeks following initial tumor formation. The combination of decitabine and navitoclax significantly reduced tumor volume (Fig. 7B) and tumor mass (Supplementary Fig. S6B) compared with either agent alone. No overt toxicities were observed.

Discussion

We profiled a panel of 45 solid tumor cell lines in ovarian, melanoma, and breast cancer lineages for their response to decitabine over a 9-day period. We demonstrated that decitabine shows pronounced time-dependent activity in a subset of solid tumor cancer cell lines. For example, activity of decitabine in OVCAR8, an ovarian cancer cell line, improved approximately 1,000-fold from 3 days of treatment ($IC_{50}^{day\ 3}$, > 33.3 μmol/L) to 9 days of treatment ($IC_{50}^{day\ 9}$, 22.2 nmol/L). Overall, decitabine demonstrated activity at low doses (IC_{50} < 150 nmol/L) in a subset of solid tumor-derived cancer cell lines and elicited a large dynamic range in sensitivity (10 nmol/L > IC_{50} > 10 μmol/L) in all lineages. In contrast, a panel of hematopoietic cell lines showed a similar range of sensitivities to decitabine after 3 days of treatment (data not published). The maximum concentration (C_{max}) of decitabine achieved in human plasma in response to low-dose decitabine treatment is 0.3 to 1.6 μmol/L (24). Given the sensitivity of a subset of solid tumors to decitabine (IC_{50} < 150 nmol/L), these data suggest that a prolonged, low-dose treatment regimen may benefit patients with some solid tumors.

To understand if decitabine's activity was stronger in certain cancer contexts, we correlated compound sensitivity to cell-line features. The absence of confounding correlations to lineage or doubling time enabled us to conduct an unbiased search for genomic features and activated pathways that are associated with sensitivity to decitabine. Genomic alterations in *KRAS*, *NRAS*, and *CRAF* as well as activation of the RAS/RAF/MEK pathway significantly correlated with sensitivity to decitabine. In addition, cell-cycle regulation correlated with sensitivity to decitabine. This pathway was previously shown to associate strongly with *KRAS* activation (30, 31).

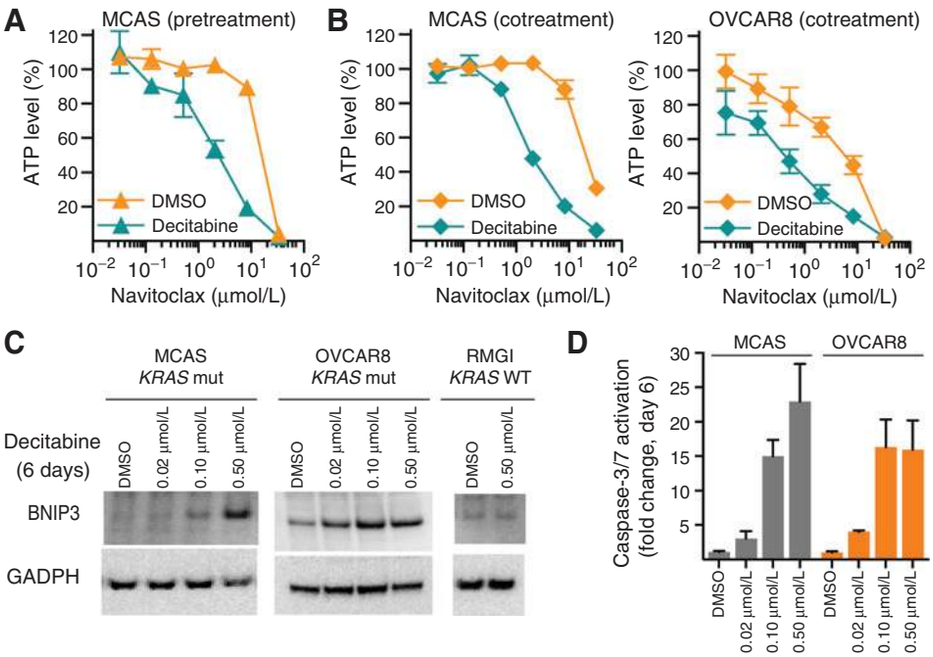

Figure 6.
Decitabine modulates activity of the BCL-2 family inhibitor navitoclax. A, *KRAS*-mutant ovarian cancer cell line, MCAS, was pretreated with decitabine for 3 days, followed by cotreatment with decitabine and navitoclax for 3 days (two biological replicates; mean ± SD). Data were normalized to the ATP levels (CTG) measured for the corresponding DMSO- or decitabine-treated controls (6 days). Data are representative of two independent experiments. B, *KRAS*-mutant ovarian cancer cell lines, MCAS and OVCAR8, were cotreated with decitabine and navitoclax for 6 days (two biological replicates; mean ± SD). Data were normalized to the ATP levels (CTG) measured for the corresponding DMSO- or decitabine-treated controls (6 days). Data are representative of two independent experiments. C, BNIP3 was probed by Western blot after treatment with decitabine for 6 days in *KRAS*-mutant (MCAS and OVCAR8) and *KRAS* wild-type (RMGI) ovarian cancer cell lines. D, caspase-3 and -7 activation was measured after 3, 6, and 9 days of treatment in *KRAS*-mutant ovarian cancer cell lines (six replicates; mean ± SD). Data are representative of two independent experiments.

Given the correlation of RAS/RAF/MEK pathway activation and decitabine activity, we tested the ability of *KRAS* genomic status to predict sensitivity to decitabine *in vitro*. *KRAS* mutations occur in 30% of low-grade serous ovarian cancers, and genomic amplifications of *KRAS* occur in 11% of high-grade serous ovarian cancer tumors (32). Six additional *KRAS*-mutant and -amplified ovarian cancer cell lines representing low- and high-grade serous ovarian cancer lines showed sensitivity to decitabine at low dose ($IC_{50} < 150$ nmol/L). These data suggest that *KRAS* genomic status may serve as a potential biomarker for sensitivity to decitabine in ovarian cancer.

RAS/RAF/MEK signaling is reported to regulate DNMT1 and DNMT1-dependent DNA methylation (20–22, 33). Specifically, overexpression of RAS has been shown to increase DNMT1 protein levels (28), and inhibition of MEK by siRNA or small-molecule inhibitors decreased expression of DNMT1 (22). In accordance with our observation that decitabine sensitivity associated with RAS pathway activation, we observed that high gene expression of *DNMT1*, but not other DNA methyltransferases, correlated with sensitivity to decitabine. We further showed that inhibition of RAS/RAF/MEK signaling with the MEK inhibitor selumetinib decreased DNMT1 levels in *KRAS*-mutant ovarian cancer cell lines. The observed data align with the reported RAS-DNMT1 signaling pathway and imply that targeting DNA methyltransferases in RAS-activated cancers may be a useful therapeutic strategy.

The activity of compounds in the presence or absence of decitabine may provide mechanistic insight into the impact of KRAS signaling on decitabine activity. For example, the combination of decitabine and vorinostat are reported to induce synergistic activity attributed to the combined disruption of chromatin marks (23). This combination has provided a platform for clinical translation (23, 34, 35). We performed compound profiling in 34 solid tumor–derived cell lines with varying sensitivities to decitabine. Given our observation that pretreatment with decitabine altered the activity of vorinostat, we profiled the response of 38 small molecules after pretreatment with decitabine for nine days. We observed that decitabine altered the activity of select compounds targeting a subset of biological pathways, including RAS/RAF/MEK signaling and BCL-2 family proteins.

Interestingly, decitabine substantially decreased activity of MEK inhibitors in *KRAS*-mutant ovarian cancers. Re-activation of the MEK/ERK pathway has been implicated in resistance to BRAF and MEK inhibitors (26) and may account for the altered activity of MEK inhibitors. Indeed, decitabine activated the MEK/ERK pathway, as indicated by increased phosphorylation of MEK and ERK. Previous studies show that activation of the MEK/ERK pathway increases proapoptotic BCL-2 family members, such as BNIP3 (27–29). The increased expression of this proapoptotic BCL-2 protein may contribute to the increased activity of the BCL-2 family inhibitor navitoclax after pretreatment with decitabine. Consistent with these findings, we found that treatment with decitabine increased BNIP3 protein levels in two *KRAS*-mutant ovarian cancer cell lines and activated caspase-3 and -7 at time points corresponding to a reduction in cell viability. Together,

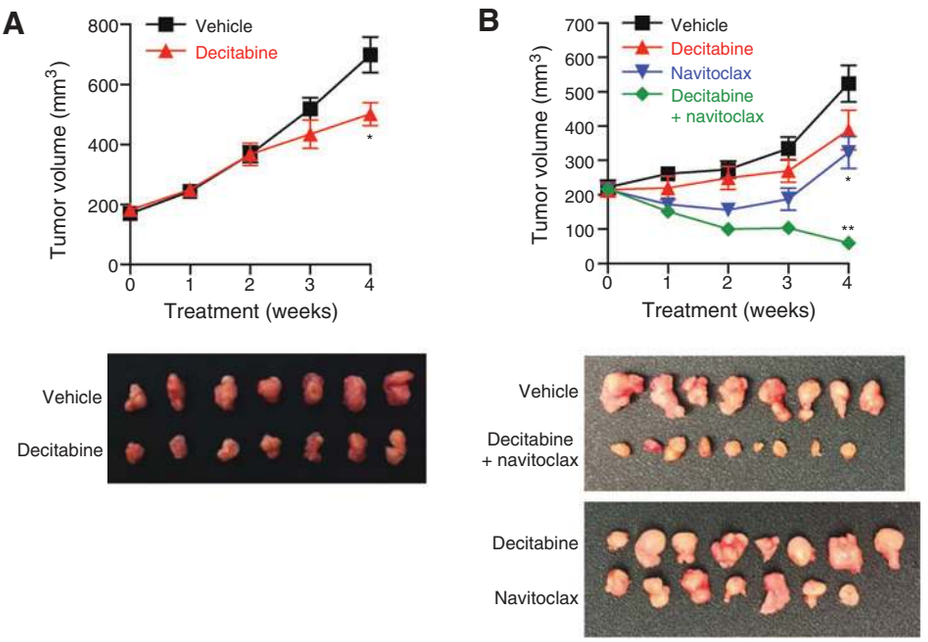

Figure 7.
The combination of decitabine and navitoclax shows activity in a xenograft mouse model derived from a *KRAS*-mutant ovarian cancer cell line. A, tumor volume as measured by caliper of low-dose decitabine (20 mg/kg, s.c., 3× per week) or vehicle administered for 4 weeks in a subcutaneous xenograft model using a *KRAS*-mutant cell line (OVCAR8; *, $P = 0.02$; Mann–Whitney). Tumors were excised after 4 weeks of treatment. B, tumor volume as measured by caliper of low-dose decitabine (0.2 mg/kg s.c., 3× per week), navitoclax (100 mg/kg i.p., 5× per week), or vehicle administered alone or in combination for 4 weeks in a subcutaneous xenograft model using a *KRAS*-mutant cell line (OVCAR8; *, $P < 0.03$; *t* test; **, $P < 0.001$; *t* test). Week 4 treatment omitted one injection of decitabine and two injections of navitoclax. Tumors were excised after 4 weeks of treatment.

these data suggest that upregulation of the MEK/ERK pathway and proapoptotic BCL-2 family proteins by decitabine contributes to reduced viability in RAS-activated cell lines and provides a rationale for the combination of decitabine and navitoclax in *KRAS*-mutant ovarian cancers.

We extended the observed cellular activity of decitabine and navitoclax to an *in vivo* xenograft model using a *KRAS*-mutant ovarian cancer cell line. We demonstrated that cotreatment with decitabine and navitoclax dramatically decreased tumor volume compared with administration of either agent alone. Further studies using multiple *KRAS*-mutant and *KRAS* wild-type ovarian cancer cell lines in diverse *in vivo* settings are necessary to account fully for the effect of tumor heterogeneity and genotype heterogeneity on the efficacy of decitabine.

Precision medicine aspires to match cancer therapeutics to patients most likely to benefit from the treatment. We have shown that RAS/RAF/MEK pathway activation correlates with sensitivity to decitabine, a small molecule traditionally used in hematologic cancers that may also have benefit in solid tumors. Cell-line and compound profiling revealed a direct role of RAS/MEK/DNMT1 signaling and the BCL-2 family of proteins in mediating sensitivity to decitabine. We showed that *KRAS* mutations or amplifications predicted sensitivity to decitabine in ovarian cancer cell lines and suggest a potential biomarker for patient stratification. Further studies are necessary to test the therapeutic benefit of these strategies in preclinical models and ultimately in patients.

Disclosure of Potential Conflicts of Interest

No potential conflicts of interest were disclosed.

Authors' Contributions

Conception and design: M.L. Stewart, S. Wang, D. Khabele, A.F. Shamji, S.L. Schreiber
Development of methodology: M.L. Stewart, P. Tamayo, S. Wang, Y.M. Chang
Acquisition of data (provided animals, acquired and managed patients, provided facilities, etc.): M.L. Stewart, A.J. Wilson, S. Wang, J.W. Kim, D. Khabele
Analysis and interpretation of data (e.g., statistical analysis, biostatistics, computational analysis): M.L. Stewart, P. Tamayo, A.J. Wilson, S. Wang, Y.M. Chang, J.W. Kim, D. Khabele, A.F. Shamji
Writing, review, and/or revision of the manuscript: M.L. Stewart, Y.M. Chang, D. Khabele, A.F. Shamji, S.L. Schreiber
Administrative, technical, or material support (i.e., reporting or organizing data, constructing databases): M.L. Stewart, S. Wang, D. Khabele
Study supervision: D. Khabele, A.F. Shamji, S.L. Schreiber
Other (performed experiments): Y.M. Chang

Acknowledgments

The authors gratefully acknowledge the following colleagues for providing a wonderfully collaborative environment and valuable comments: Drs. J.S. Boehm, W.C. Hahn, and J.P. Mesirov. They also thank the following colleagues for their thoughtful discussions and critique: Drs. J. Kotz, D. Adams, A. Basu, N.E. Bodycombe, S. Chattopadhyay, J.H. Cheah, P.A. Clemons, C. Hon, C. Johannessen, E.H. Leshchiner, M. Rees, G.I. Schaefer, B. Seashore-Ludlow, A.M. Stern, and V. Sridhar. They thank the Biological Samples Platform for providing the cancer cell lines. The project was enabled by the Cancer Target Discovery and Development Centers at the Broad Institute and Dana-Farber Cancer Institute and the Broad Institute Center for the Science of Therapeutics. The authors are grateful for the leadership of the CTD^2 Network by Daniela Gerhard (Director, Office of Cancer Genomics, NCI). S.L. Schreiber is an Investigator at the Howard Hughes Medical Institute.

Grant Support

This work was supported by the NCI's Cancer Target Discovery and Development grant (U01CA176152, awarded to S.L. Schreiber) and an NCI Career Development Award (K08CA148887, awarded to D. Khabele).

The costs of publication of this article were defrayed in part by the payment of page charges. This article must therefore be hereby marked *advertisement* in accordance with 18 U.S.C. Section 1734 solely to indicate this fact.

Received September 25, 2014; revised April 9, 2015; accepted April 28, 2015; published OnlineFirst May 12, 2015.

References

1. Barton CA, Hacker NF, Clark SJ, O'Brien PM. DNA methylation changes in ovarian cancer: implications for early diagnosis, prognosis and treatment. Gynecol Oncol 2008;109:129–39.
2. Cowan LA, Talwar S, Yang AS. Will DNA methylation inhibitors work in solid tumors? A review of the clinical experience with azacitidine and decitabine in solid tumors. Epigenomics 2010;2:71–86.
3. Esteller M. Epigenetics in cancer. N Engl J Med 2008;358:1148–59.
4. Kantarjian H1, Oki Y, Garcia-Manero G, Huang X, O'Brien S, Cortes J, et al. Results of a randomized study of 3 schedules of low-dose decitabine in higher-risk myelodysplastic syndrome and chronic myelomonocytic leukemia. Blood 2007;109:52–7.
5. Sharma SV, Haber DA, Settleman J. Cell line-based platforms to evaluate the therapeutic efficacy of candidate anticancer agents. Nat Rev Cancer 2010;10:241–53.
6. Basu A, Bodycombe NE, Cheah JH, Price EV, Liu K, Schaefer GI, et al. An interactive resource to identify cancer genetic and lineage dependencies targeted by small molecules. Cell 2013;154:1151–61.
7. Garnett MJ, Edelman EJ, Heidorn SJ, Greenman CD, Dastur A, Lau KW, et al. Systematic identification of genomic markers of drug sensitivity in cancer cells. Nature 2012;483:570–5.
8. Barretina J, Caponigro G, Stransky N, Venkatesan K, Margolin AA, Kim S , et al. The Cancer Cell Line Encyclopedia enables predictive modelling of anticancer drug sensitivity. Nature 2012;483:603–7.
9. Kim W, Bird GH, Neff T, Guo G, Kerenyi MA, Walensky LD, et al.. Targeted disruption of the EZH2-EED complex inhibits EZH2-dependent cancer. Nat Chem Biol 2013;9:643–50.
10. Vedadi M, Barsyte-Lovejoy D, Liu F, Rival-Gervier S, Allali-Hassani A, Labrie V, et al. A chemical probe selectively inhibits G9a and GLP methyltransferase activity in cells. Nat Chem Biol 2011;7:566–74.
11. Adams DJ, Dai M, Pellegrino G, Wagner BK, Stern AM, Shamji AF, et al. Synthesis, cellular evaluation, and mechanism of action of piperlongumine analogs. Proc Natl Acad Sci U S A 2012;109: 15115–20.
12. Joe H. Relative Entropy Measures of Multivariate Dependence. J Am Stat Assoc 1989;84:157–64
13. Wood KC, Konieczkowski DJ, Johannessen CM, Boehm JS, Tamayo P, Botvinnik OB, et al. MicroSCALE screening reveals genetic modifiers of therapeutic response in melanoma. Sci Signal 2012;5:rs4.20.
14. Liberzon A, Subramanian A, Pinchback R, Thorvaldsdóttir H, Tamayo P, Mesirov JP. Molecular signatures database (MSigDB) 3.0. Bioinformatics 2011;27:1739–40.
15. Abe T, Toyota M, Suzuki H, Murai M, Akino K, Ueno M, et al. Upregulation of Bnip3 by 5-aza-2′-deoxycytidine sensitizes pancreatic cancer cells to hypoxia-mediated cell death. J Gastroenterol 2005;40: 504–10.
16. Ellinger-Ziegelbauer H, Kelly K, Sienbenlist U. Cell cycle arrest and reversion of Ras-induced transformation by conditionally activated form of mitogen-activated protein kinase kinase kinase 3. Mol Cell Biol 1999;19: 3857–68.
17. Chen G, Hitomi M, Han J, Stacey DW. The p38 pathway provides negative feedback for Ras proliferative signaling. J Biol Chem 2000;275: 38973–80
18. Barbie DA, Tamayo P, Boehm JS, Kim SY, Moody SE, Dunn IF , et al. Systematic RNA interference reveals that oncogenic KRAS-driven cancers require TBK1. Nature 2009;462:108–12.
19. Bell D, Berchuck A, Birrer M, Chien J, Cramer D, Dao F, et al. Integrated genomic analyses of ovarian carcinoma. Nature 2012;490:609–15.
20. Gazin C, Wajapeyee N, Gobeil S, Virbasius CM, Green MR. An elaborate pathway required for Ras-mediated epigenetic silencing. Nature 2007; 449:1073–7.
21. Wajapeyee N, Malonia SK, Palakurthy RK, Green MR. Oncogenic RAS directs silencing of tumor suppressor genes through ordered recruitment of transcriptional repressors. Genes Dev 2013;27:2221–6.
22. Lu R, Wang X, Chen ZF, Sun DF, Tian ZQ, Fang JY. Inhibition of the extracellular signal-regulated kinase/mitogen-activated protein kinase pathway decreases DNA methylation in colon cancer cells. J Biol Chem 2007;282:12249–59.
23. Stathis A, Hotte SJ, Chen EX, Hirte HW, Oza AM, Moretto P, et al. Phase I study of decitabine in combination with vorinostat in patients with advanced solid tumors and non-Hodgkin's lymphomas. Clin Cancer Res 2011;17:1582–90.
24. Cashen AF, Shah AK, Todt L, Fisher N, DiPersio J. Pharmacokinetics of decitabine administered as a 3-h infusion to patients with acute myeloid leukemia (AML) or myelodysplastic syndrome (MDS). Cancer Chemother Pharmacol 2008, 61:759–766.
25. Alcazar O, Achberger S, Aldrich W, Hu A, Negrotto S, Saunthararajah Y, et al. Epigenetic regulation by decitabine of melanoma differentiation *in vitro* and *in vivo*. Int J Cancer 2012;131:18–29.
26. Little AS, Smith PD, Cook SJ. Mechanisms of acquired resistance to ERK1/2 pathway inhibitors. Oncogene 2013;32:1207–15.
27. An JH, Lee H, Paik SG. Silencing of BNIP3 results from promoter methylation by DNA methyltransferase 1 induced by the mitogen-activated protein kinase pathway. Mol Cells 2011;31:579–83.
28. An JH, Maeng O, Kang KH, Lee JO, Kim YS, Paik SG, et al. Activation of Ras up-regulateds pro-apoptoic BNIP3 in nitric oxide-induced cell death. J Biol Chem 2006;281:33939–48.
29. Kalas W, Swiderek E, Rapak A, Kopij M, Rak J, Strzadala L. H-ras upregualates expression of BNIP3. Anticancer Res 2011;m31:2869–75.
30. Ng KP1, Ebrahem Q, Negrotto S, Mahfouz RZ, Link KA, Hu Z , et al. p53 independent epigenetic-differentiation treatment in xenotransplant models of acute myeloid leukemia. Leukemia 2011;25:1739–50.
31. Luo J, Emanuele MJ, Li D, Creighton CJ, Schlabach MR, Westbrook TF, et al. A genome-wide RNAi screen identifies multiple synthetic lethal interactions with the Ras oncogene. Cell 2009;137:835–848.
32. Domcke S, Sinha R, Levine DA, Sander C, Schultz N. Evaluating cell lines as tumour models by comparison of genomic profiles. Nat Commun 4:2126.
33. Pakneshan P, Szyf M, Rabbani SA. Methylation and inhibition of expression of uPA by the RAS oncogene: divergence of growth control and invasion in breast cancer cells. Carcinogenesis 2005;26:557–664.
34. Matei DE, Nephew KP. Epigenetic therapies for chemoresensitization of epithelial ovarian cancer. Gynecol Oncol 2010;116:195–201.
35. Matei D, Fang F, Shen C, Schilder J, Arnold A, Zeng Y , et al. Epigenetic resensitization to platinum in ovarian cancer. Cancer Res 2012;72: 2197–205.